Inverse cascades in turbulence and the case of rotating flows

2013 Phys. Scr. 2013 014032

(http://iopscience.iop.org/1402-4896/2013/T155/014032)

Phys. Scr. **T155** (2013) 014032 (10pp) doi:10.1088/0031-8949/2013/T155/014032

Inverse cascades in turbulence and the case of rotating flows

A Pouquet[1], A Sen[1], D Rosenberg[1], P D Mininni[1,2] and J Baerenzung[3]

[1] Computational and Information Systems Laboratory, NCAR, PO Box 3000, Boulder, CO 80307, USA
[2] Departamento de Física, Facultad de Ciencias Exactas y Naturales, UBA and IFIBA, CONICET, Ciudad Universitaria, 1428 Buenos Aires, Argentina
[3] Interdisciplinary Center for Dynamics of Complex Systems, D-14476 Potsdam, Germany

E-mail: pouquet@ucar.edu

Received 29 February 2012
Accepted for publication 12 May 2012
Published 16 July 2013
Online at stacks.iop.org/PhysScr/T155/014032

Abstract
We first summarize briefly several properties concerning the dynamics of two-dimensional (2D) turbulence, with an emphasis on the inverse cascade of energy to the largest accessible scale of the system. In order to study a similar phenomenon in 3D turbulence undergoing strong solid-body rotation, we test a previously developed large eddy simulation (LES) model against a high-resolution direct numerical simulation of rotating turbulence on a grid of 3072^3 points. We then describe new numerical results on the inverse energy cascade in rotating flows using this LES model and contrast the case of 2D versus 3D forcing, as well as non-helical forcing (i.e. with weak overall alignment between velocity and vorticity) versus the fully helical Beltrami case, for both deterministic and random forcing. The different scaling laws for the inverse energy cascade can be attributed to the dimensionality of the forcing, with either a $k_\perp^{-3}$ or a $k_\perp^{-5/3}$ energy spectrum of slow modes at large scales, $k_\perp$ referring to a direction perpendicular to that of rotation. We finally invoke the role of shear in the case of a strongly anisotropic deterministic forcing, using the so-called ABC flow; in that case, a $k_\perp^{-5/3}$ is again observed for the slow modes, together with a k^{-1} spectrum for the total energy associated with enhanced shear at a large scale [92].

PACS numbers: 47.32.Ef, 47.27.−i, 47.27.ek

(Some figures may appear in color only in the online journal)

1. Introduction

The interactions between winds and waves (mostly surface gravity waves) have an important role in planetary and oceanic boundary layers with dynamical consequences for mixing, in particular the upper layer of the ocean, affecting the momentum, heat and CO_2 transport. For example, this may result in a Southern Ocean mixed layer, which is too shallow in many climate models [41], thereby affecting the overall climate evolution [20]. These difficulties with global models, for both climate dynamics and weather prediction, can be related to inadequacies in the numerical treatment of wave breaking, as it manifests itself in overturning and Kelvin–Helmoltz instabilities, because of insufficient resolution. This leads in turn to the inaccurate modeling of nonlinear interactions which take over both at small scales, with enhanced turbulent mixing, dissipation and intermittency, i.e. the occurrence of localized extreme events, and at large scales in the form of inverse cascades.

Non-equilibrium turbulent processes are ubiquitous in our environment, and they can be tackled in a unified framework using an array of statistical tools, although it is expected and observed that temporal evolutions, scaling laws and physical structures display a variety of different behaviors. Enhanced dissipation and mixing, as observed in many instances in geophysical flows such as oceans (see, e.g. [50]), can be quantified in laboratory experiments, in numerical simulations and in observations of geophysical flows. For example, simultaneous data on small-scale buoyancy, shear and dissipation collected in an Arctic fjord [39] give us a more accurate understanding of the interactions between turbulent eddies and waves, with an

evaluation of eddy diffusivity as a function of the Richardson number. Such detailed observations can also lead to an assessment of parameterization models of small-scales eddies as they appear in current weather and climate codes.

Among such complex flows, two-dimensional (2D) flows play a special role, be it only because they are more amenable to numerical simulations at high resolution. The present renewed interest in 2D turbulence is due to several factors. On the one hand, the increased power of computers allows for modeling flows with higher Reynolds numbers and thus for a more accurate determination of the statistics and characteristics of such flows. Moreover, the observation in the atmospheric boundary layer of an energy spectrum with a k^{-3} law followed at smaller scales by a $k^{-5/3}$ law [79] has led to some controversy since the opposite case was believed to happen (see below): the atmosphere is viewed as quasi-2D at large scales, as a recent analysis of data with modern velocimetry techniques shows rather unambiguously [44], and thus is expected to undergo an inverse cascade of energy to large scales.

The inverse energy cascade in 2D flows was first observed numerically [48]. It was later confirmed experimentally in [99] using an electrically driven flow in a thin layer of mercury in a square box, and in numerous configurations after these pioneering papers [13, 101]. There are other 2D systems undergoing inverse cascades when incorporating more physical phenomena, such as beta-plane turbulence or multi-layer quasi-geostrophic (QG) flows [67, 106], as well as when coupling the velocity dynamics to that of magnetic induction (although in the case of conducting fluids, it is not the energy that populates the scales larger than the forcing scale). For very strong rotation (at a fixed Reynolds number) it is known that 3D flows tend to become 2D and thus to remain non-singular in the limit of zero viscosity [1]; indeed, an inverse cascade of energy was observed in [96] for such flows, and the co-existence of an inverse cascade of energy to large scales and of a direct cascade of energy (and of helicity) to small scales was studied in [71, 72] (see [88] for a recent review), with the eventual recovery of isotropy and Kolmogorov scaling at small scales [73].

The inverse cascade of energy in 2D turbulence was postulated by Onsager [38, 83] when studying the interactions of an ensemble of point vortices and by Kraichnan [55] using statistical equilibria of a finite number of degrees of freedom in the ideal (non-dissipative) case. This cascade is characterized by a transfer of energy with a constant flux, up to the largest scale accessible to the system; it is attributed to the dual constraint of total energy and squared vorticity (enstrophy) conservation for inviscid 2D flows. The review paper by Kraichnan and Montgomery [59] on 2D turbulence focused on theoretical issues, including those in the case of coupling to a magnetic field. It states that the inverse cascade for 2D fluids should follow an $E(k) \sim k^{-5/3}$ spectrum (similar to the Kolmogorov spectrum in the direct cascade of energy in three dimensions), together with a k^{-3} law for the energy in the direct enstrophy cascade to small scales [3, 18, 27, 62, 104]. Steeper spectra at a small scale have been observed [14, 108], in particular in early numerical simulations at low resolution; sometimes they are related to the dominance in such computations of strong coherent vortices.

In physical space, the inverse cascade corresponds to the formation of large-scale vortices (jets [34] or bars [116] can also be found). These structures have been observed for quite a while in numerical simulations [48] and in the laboratory [99]. They can be viewed as caused by a negative eddy viscosity arising from small-scale eddies [58], or as a non-local interaction between a small-scale vortex embedded in a large-scale strain [28]. However, it has also been known for a long time that large-scale spectra can be steeper than $k^{-5/3}$, especially close to the gravest allowable mode where the energy condenses. In this case, long-time energy accumulation at the largest scale is viewed as providing a source of energy for a downward cascade to smaller scales through filamentation of the large-scale vortex. The large-scale flow can, in turn, decrease the level of turbulence [94], as also found in the context of plasma flows [10]. When Ekman friction is present, steeper spectra in inverse cascades can also be interpreted as caused by a wavenumber-dependent energy flux arising from the friction, similar to a phenomenon already documented for magnetohydrodynamic flows in the quasi-static approximation relevant at low magnetic Reynolds numbers [109]. Furthermore, it is shown in [24] that the saturation time of the inverse cascade scales as ν^{-1} and that the saturation level of the energy, which depends on both the force and the dissipation, needs a well-resolved enstrophy range, due to non-local interactions between small scales and large scales. It is also worth noting that, in a reduced model of the rotating Rayleigh–Bénard convection, the authors of [51] found that a k^{-3} for the spectrum of the horizontal energy takes place in an inverse cascade for late times.

These so-called condensates undergo random reversals, more temporally sparse when large-scale friction is diminished, the coupling to high-frequency modes providing the random noise that can trigger the transition from one large-scale quasi-steady state to another [35]; this phenomenon is observed in Rayleigh–Bénard convection, in 2D Navier–Stokes turbulence in boxes with a close to unity aspect ratio [15], in fluid experiments [66], in dynamo experiments [4] and in the reversal of the Kuroshio oceanographic current [89] and of the magnetic field of the Earth [105].

The turbulence statistics in the inverse cascade is Gaussian until the formation of the condensate, when the spectrum steepens [95]: the inverse cascade is known to be self-similar, with a linear variation with the order of scaling exponents of structure functions of the velocity field. However, Smith and Yakhot [95] noted that the condensate is responsible for intermittency at a large scale, viewed as a finite-size effect due to the fact that the inverse cascade of energy has reached the gravest mode, and the boundary of the system where (Ekman) friction can play a role as well. Intermittency in an inverse cascade was diagnosed at high-order statistics in [52] in a soap-film experiment. A balance between linear friction $\sim\alpha\mathbf{u}$ and advection $\mathbf{u}\cdot\nabla\mathbf{u}$ gives $E(k) \sim k^{-3}$ but possibly in the absence of a constant flux of energy, since friction acts at all scales in the inverse cascade range. Moreover, removing the large-scale large-intensity vortices leads to recovery in the inverse range of a $k^{-5/3}$ law again, linking clearly the change in spectral slope to

the presence or absence of coherent structures. The origin of these coherent structures has been studied in the context of relaxation processes for long times and of entropy principles (see, e.g. [19, 70, 78, 93] and also [90] for surface QG flows and the case of a passive tracer in such a 2D turbulence).

2. Inverse cascades

2.1. Forcing and dissipation mechanisms and the lack of universality in 2D flows

In a series of experiments, it was found that, depending on the bottom-wall friction, two different regimes could be observed: for weak forcing, a condensate forms via the merging of smaller vortices, with a steep $\sim k^{-3}$ spectrum, whereas for strong forcing, a $k^{-5/3}$ cascade is observed with clustering of vortices at a size comparable to that of the forcing scale [84]. The influence of the large-scale drag on the inverse cascade and on structure formation was also investigated in [100]. From the numerical standpoint, the analysis of such spectral laws shows that they depend also on whether or not both the direct and inverse ranges are properly resolved [34, 91]; as an example, hyperviscosity and a short enstrophy range inhibit the formation of the large-scale vortex and thus favor a $k^{-5/3}$ law. Furthermore, disruption of vortices into filaments can happen only when the small-scale range (to which the filaments belong) is sufficiently well resolved, in turn affecting the steepness of the resulting energy spectrum [107]. There are also some indications that, when the Reynolds number is increased sufficiently so that an enstrophy cascade develops, the spectrum of the inverse energy cascade steepens, a phenomenon again related to the more efficient formation of large-scale coherent structures [91].

Some degree of non-universality in the structures and statistics of the flow has thus been observed due to several factors: the nature of the forcing term, the friction (or hypo-viscosity) used at a large scale to prevent an accumulation of energy on the gravest mode, the eventual dissipation mechanism at small scales, as well as boundary conditions and the overall geometry (see, e.g. [17, 25, 37]). As an example of the latter factor, it was shown analytically in [25] that a single vortex forms in a square domain, but a dipole forms for rectangular boxes of sufficient aspect ratio (greater than $\approx$1.12). It was also found in [17] that the correlation time of the forcing function matters in determining the shape of vortices, although very long time statistics are needed in order to observe the effect.

The observed correlation between small- and large-scale dynamics implies non-locality in Fourier space and non-universality [34], and also implies that both cascade ranges have to be explicitly incorporated into the flow, with sufficient resolution at small and large scales. Non-local interactions seem to be particularly evident when polymers are added to the flow: they affect the small scales and produce a drag reduction, but are also known to affect the inverse cascade of energy at large scale; this was shown using a shell model [6] and in experiments [53]. Another example of scale non-locality comes from the recent study in [17], where the statistics of vortex population was analyzed. However, it should be noted that a wavelet-based analysis of 2D turbulence was performed in [40], concluding that enstrophy transfer is local in configuration space.

In recent years, higher resolutions have been achieved in 2D simulations [7, 11, 17, 107], with up to $32\,768^2$ grid points, leading to sizable cascades including resolving the dual (direct and inverse) cascades, and with a choice of forcing scale of up to roughly $1/1000$ the size of the overall computational box. This has allowed for refined statistics, including a detailed study on the conformal invariance properties of the inverse cascade of energy [7]. However, whether a logarithmic correction to the small-scale spectra as predicted by Kraichnan [56], ensuring locality of interactions, is present or not is still open to debate. A moderate-resolution run with very long time integration (of the order of 1000 turnover times) and using both linear friction and hyper-viscosity finds such a correction [85], and this was found in [106] also in the case of 3D QG turbulence. On the other hand, no such correction appears in the 2D case at substantially higher resolutions (but not necessarily at higher Reynolds numbers, given the choice of forcing wavenumber) or in the absence of large-scale friction [107] (see also [65]).

2.2. The case of quasi-2D flows

The 2D fluid turbulence is thus being explored and reassessed today in view of several new results stemming mostly (but not uniquely) from direct numerical simulations (DNS), with new findings for systems that are closely related but not identical to the original 2D-2C (two-dimensional, two velocity components) case. But how much can one depart from the standard 2D-2C case and still observe an inverse cascade of energy? Indeed, the experimental flows discussed above are at best quasi-2D, so that one can ask whether the finite thickness of the fluid with which the experiments are carried out, or the existence and/or roughness of the boundary layer, play a role in the dynamics of such flows. Flows in nature, such as the atmosphere and oceans, are also quasi-2D.

This question has been tackled recently using a variety of approaches. The inverse cascade of energy in quasi-2D flows is a phenomenon already observed in the framework of shell models [12, 81]. For example, in [81], adjusting the parameters in the model allowed for a quasi-2D behavior in so far as a dual (direct/inverse) cascade was observed, and in [23], the transition from 3D to 2D behavior was attributed to a preferred transfer to $k_z = 0$ Fourier modes when rotation was imposed in the z-direction.

Recent DNS using a 2D (say, horizontal) forcing term in a 3D box with a varying aspect ratio in the vertical direction show that, already for an aspect ratio smaller than $1/2$, an inverse cascade of energy begins to develop with a linear growth of the energy [21] (see also [96]). The growth rate approaches the injection rate of energy as the aspect ratio decreases; in fact, it was found in [91] that the strength of the cascade increases in a monotonic fashion as the Reynolds number (i.e. the extent of the direct enstrophy cascade) grows. Similarly, in quasi-2D experimental flows with thick layers of fluid, it was shown in [113] that a strong planar vortex suppresses vertical eddies through vertical shear with an associated time scale that is shorter than the vertical eddy turn over time (thus enabling it to quench vertical motions),

and that small-scale and large-scale forcing can combine to form an inverse energy cascade. A similar reversal of cascade direction was found in [29] for a passive tracer embedded in a compressible flow. However, it is not clear whether a supersonic flow, as encountered for example in the interstellar medium, will reach such a degree of compressibility since shocks form and decay rapidly, whereas vortices build on an eddy turnover time [60].

Finally, the conditions under which turbulence spectra can be superposed or not when excited at two different scales and with two different rates, as can occur in the oceans for example, have been investigated in the context of two direct cascades [87] in 3D turbulence, and more recently considering the interactions of direct and inverse cascades in 2D [22].

2.3. Restricted 3D helical flows

In a traditional view of incompressible fluid turbulence, the invariants of the ideal equations (those in the absence of dissipation) determine to a large extent the dynamics of the dissipative case. If the energy invariance of an ideal 3D flow is well known, such is not necessarily the case for the other quadratic invariant—helicity—as observed, say, in the vicinity of tornadoes [32]. Helicity is defined as the correlation between the velocity $\mathbf{u}$ and its curl, the vorticity $\omega = \nabla \times \mathbf{u}$, namely $H = \int \mathbf{u} \cdot \omega \; d^3\mathbf{x}$; note that helicity is not definite positive, which renders the interpretation of its Fourier dynamics and fluxes more complex (see, e.g. [26] for a detailed analysis). A helical flow can be viewed as a superposition of helically ($s = \pm$) polarized waves [33, 45, 112] written as

$$\mathbf{u}(\mathbf{k}) = \Sigma_s a_s(\mathbf{k}) \mathbf{h}_s(\mathbf{k}), \quad \mathbf{h}_\pm(\mathbf{k}) = \hat{p} \times \hat{k} \pm \mathrm{i}\hat{p}, \quad \mathbf{p}(\mathbf{k}) = \hat{z} \times \mathbf{k},$$

with the hat defining vectors of unit length and z being an arbitrary direction, conveniently chosen in the rotating case as the axis of rotation, making the $\mathbf{h}_\pm$ functions helically polarized inertial waves. This helical wave decomposition has recently been generalized to the case of channel flows, including with streamwise rotation [115]. Note that there are four types of basic triadic interactions for wavevectors $\mathbf{k}$, $\mathbf{p}$, $\mathbf{q}$, defined by the helicity modes (s_k, s_q, s_q), namely $(s_k, s_q, s_q) = (+++)$, $(++-)$, $(+-+)$ and $(+--)$, plus four more exchanging the two (+ and −) polarities [112].

For 3D turbulence in the presence of helicity, only a dual energy and helicity cascade to small scales has been found in numerous DNS, with both following a Kolmogorov $k^{-5/3}$ law. Loosely speaking, being more of a small-scale field since it weighs more the small scales than does the energy, the helicity will undergo a direct cascade to small scale more readily than the energy does. However, and perhaps more surprisingly, an inverse cascade of energy (with a direct cascade of helicity) was observed recently for 3D helical turbulence when restricting the nonlinear interactions to the subsets of Fourier modes that have only one-sign (either + or −) polarity [9]. In the general case, waves of different signs can interact (see [111, 112]), but since individual triadic nonlinear interactions conserve the invariants separately, one can indeed truncate the equations to such subsets of modes. It is interesting to point out that when dealing with all interactions (+ and −), the helicity cascade is difficult to study as its flux may also change signs. Restricting interactions to same-sign modes does not have such an impediment, and a direct cascade of helicity can be identified clearly. The invariance of one-signed helicity in this restricted case leads to the inverse cascade of energy to large scales which follows again a $k^{-5/3}$ spectrum [9].

This result does not contradict the previous numerical findings using the full set of nonlinear interactions; indeed, it was shown in [57] that same-sign interactions are sub-dominant and thus one can recover the traditional direct cascade of energy for 3D fluid turbulence in the full case. The recent study in [9] does show, however, that the principles of statistical mechanics, on the basis of which arguments can be developed in favor of direct and inverse cascades, are sturdy and extend also, perhaps in unexpected ways, to (carefully selected) subsets of modes. Sub-ensembles of modes having different scaling laws are a known feature of turbulent flows, such as for example in Rayleigh–Bénard convection when differentiating between the (0, 0, $2n$) modes of the temperature and all other modes, due to inherent symmetries of the equations [75]. The *gedanken* numerical experiment restricting interactions to the +++ triads also gives credence to the observation that, when examining the individual energy transfer in triads, there are numerous interactions transferring energy to large scales, some of which can be interpreted as being due to this subset of same-signed helical modal interactions, and others that obviously correspond to purely 2D triads. Finally, note that a large-scale instability akin to that in magnetohydrodynamics can develop when the small scales are both helical and anisotropic [42, 64]

2.4. Decaying versus forced flows

Traditionally, inverse cascades are considered to be the hallmark of forced turbulence: forcing is viewed as necessary for observing an inverse cascade, in particular because of the energy needed to populate the large scales, with a linear growth of the total energy in time. However, it has recently been shown, using an ensemble of numerical simulations computed on grids of up to 4096^2 points, that a large-scale $k^{-5/3}$ spectrum can be observed also in the decaying case at scales larger than those of the initial conditions, k_0^{-1}, when taking the average over long times and over the ensemble [74]. This observed spectrum corresponds to an inverse cascade with a constant negative flux for the ensemble. The source of energy for this to happen comes from the fact that, at sufficiently late times, the energy at k_0 has decreased substantially, part of it being fed to larger scales. Such a behavior is not necessarily surprising since it is contained in the nonlinearity of the primitive equations but it has implications for experimental quasi-2D flows, which are found to follow in some cases a $k^{-5/3}$ law even though the flow is interpreted as being decaying.

2.5. Breakdown of 2D effects and rotating flows

The reverse effect of the selection of 2D modes in initially quasi-2D flows, or in other words, the three-dimensionalization of 2D turbulence, has also been observed, e.g., in freely decaying turbulence [82]. Similarly, forced turbulence with solid-body rotation Ω, which behaves in

a quasi-2D way at large scale, has recently been shown to recover its 3D properties at small scales [73], provided that the so-called Zeman scale $\ell_\Omega = [\epsilon/\Omega^3]^{1/2}$ with $\epsilon = \dot{E}$ (equivalent to the Ozmidov scale for stratified flows) is resolved (the Zeman and the Ozmidov scales are defined as the scales at which the turnover time and the wave period are equal). One may have to distinguish here between decaying flows, for which the Reynolds and Rossby numbers vary in time in different ways, and the forced case in which these two dimensionless parameters can be kept relatively constant. In the decaying case, the ratio of the Zeman to the dissipation scale varies with time (the Zeman scale decreasing as the Rossby number decreases), whereas in the forced case this ratio does not change substantially and could even be constrained to retain a constant value. Thus, the fact that anisotropy is found to be stronger at smaller scales in a laboratory experiment analyzed recently [61] may be related to the variation of this ratio of scales and is not necessarily in contradiction with DNS results of isotropization of the small scales in the presence of forcing (although non-monotonic effects in rotating flows cannot be discarded either). Again, universality should not be assumed too rapidly when several phenomena with different time scales are in competition, and more experiments, both numerical and in the laboratory, are clearly needed.

What remains of these findings in the presence of the imposed solid-body rotation? Of course, the computational demand is substantially greater than in 2D, and it will take time to explore the parameter space thoroughly, but results are already emerging that stress the role played by the nature of the forcing (emphasizing or not 2D versus 3D modes) at large scales [97]. It is in this context that we wish to address briefly the extent to which sub-grid scale models of turbulence can be used to further explore the parameter space in rotating turbulence. To this end, we present here new tests of a previously developed large eddy simulation (LES) model of turbulence [2], for which the Zeman scale may or may not be resolved against a rotating turbulence DNS performed on a grid of 3072^3 points, for which the Zeman scale is well resolved. We then mention recent results on the inverse cascade of energy in rotating 3D turbulence using this model, and end the paper with some concluding remarks.

3. Resolving or not the Zeman scale in a model of rotating turbulence

Let us begin by writing the incompressible Navier–Stokes equations in a rotating frame of reference:

$$\frac{\partial \mathbf{u}}{\partial t} + \boldsymbol{\omega} \times \mathbf{u} + 2\Omega \times \mathbf{u} = -\nabla \mathcal{P} + \nu \nabla^2 \mathbf{u} + \mathbf{F}; \quad \nabla \cdot \mathbf{u} = 0; \quad (1)$$

$\mathcal{P}$ is the pressure modified by the centrifugal term, obtained by taking the divergence of equation (1); rotation $\boldsymbol{\Omega}$ is imposed in the vertical (z) direction. The Reynolds number $Re = U_0 L_F/\nu$ with U_0 being the rms velocity, $L_F = 2\pi/k_F$ the forcing scale and ν the kinematic viscosity; $Ro = U_0/(2L_F\Omega)$ is the Rossby number; $\mathbf{F}$ is a forcing term.

Together with energy, helicity is an invariant of the Euler equations (see [76] for a review) including in the presence of solid-body rotation. In Fourier space, the relative helicity is $\rho(k) = H(k)/[2kE(k)]$ with $H = \int H(k)\mathrm{d}k$ and $E = \int E(k)\mathrm{d}k$ the total energy. A Schwarz inequality implies that $|\rho(k)| \leqslant 1$, and the helicity is said to be maximal when $\rho(k) = \pm 1$. It can be created locally in space through the correlation of vorticity and shear or pressure gradients [69] and globally through a combination of stratification and boundaries or rotation [76]. Fully helical (Beltrami) flows, with aligned velocity and vorticity everywhere, can be represented by the so-called ABC flow [31]:

$$\mathbf{u}/u_0 = [B\cos(k_0 y) + C\sin(k_0 z)]\hat{x} + [C\cos(k_0 z) + A\sin(k_0 x)]\hat{y} + [A\cos(k_0 x) + B\sin(k_0 y)]\hat{z}. \quad (2)$$

Such flows are not attractors of statistical ensembles in ideal fluids [57] and are not globally stable [86], but, in helical turbulent flows in the absence of rotation, full mirror-symmetry (no helicity) recovers slowly with wavenumber, as $1/k$, since both the energy and the helicity have Kolmogorov $k^{-5/3}$ spectra. Note that the ABC flow is an intrinsically 3D flow; it excites only a few modes selected by its helical symmetry in a given shell (basically along the three k_x, k_y and k_z axes), with dependence in all three directions, and has three components of the velocity field. However, the amount of energy in 2D versus 3D modes remains constant when one increases k_0. On the other hand, for isotropic initial conditions or forcing, the amount of energy in 2D versus 3D modes decreases when one increases the wavenumber of the flow since the energy in the 2D modes grows as k_0, while the energy in 3D modes grows as k_0^2, i.e. as the number of points in a spherical Fourier shell. When the ABC flow is concentrated at the large scales, the resulting anisotropy of the flow is not significant, but for problems of energy decay [103], or for inverse cascades for which ABC is used as a forcing and is moved to small scales with forcing wavenumber $k_F = k_0$ of the order of a few tens, the anisotropy becomes measurable and can affect the resulting dynamics [92].

The DNS of forced rotating turbulence used as the 'ground truth' to validate the LES results corresponds to a simulation with 3072^3 points, with parameters $Ro = 0.07$ and $Re = 2.7 \times 10^4$, chosen such that the Zeman scale is well resolved ($k_\Omega \approx 30$). ABC was used as the forcing $\mathbf{F}$ to inject both energy and helicity, and was applied at $k_F = k_0 = 4$. The LES we employ is described in detail in [2]; it has been tested against a DNS on a grid of 1536^3 points with forcing at $k_F = 7$ that has the Zeman scale close to the dissipation scale. The LES model implements both an eddy viscosity and an eddy noise, and these two transport coefficients have both a non-helical and a helical contribution. The eddy viscosity does not assume a Kolmogorov spectrum but rather fits the spectrum at a given time with a power law followed by an exponential decay; the fit is done in the interval $[k_c/3, k_c]$, where k_c is the cut-off wavenumber. Hence the question arises as to whether the LES can capture the behavior of the Zeman scale when this scale lies in the middle of the inertial range. We thus look at several LES runs computed on grids of 128^3 to 512^3 points. All flows start from the same initial conditions, a statistically steady state of a turbulent flow without rotation and thus have initially Kolmogorov spectra both for the energy and the helicity.

Figure 1 (top) shows the temporal evolution of the total kinetic energy and of the energy injection rate for the DNS

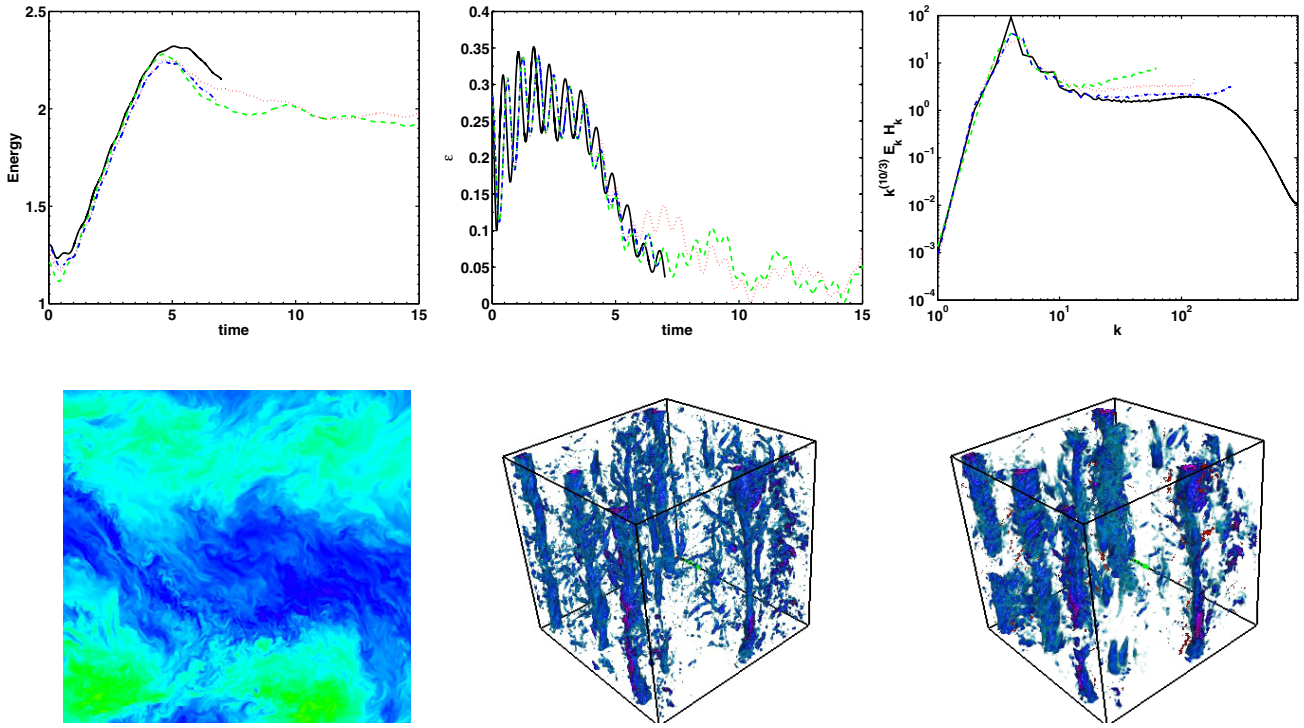

Figure 1. Top: time evolution, for $\Omega = 5$, of the energy E (left) and its input rate ϵ (middle left) for the DNS on a grid of 3072^3 points (black) and for LES runs (128^3, green dash; 256^3, red dots; and 512^3, blue dash-dot). Right: product of the energy and helicity spectra compensated for by $k^{10/3}$ for the same runs and averaged for $t \in [4.5, 6.5]$. Bottom: visualizations of the 3072^3 DNS run. Left: 2d cut of the vertical velocity. Perspective rendering of the rms vorticity (middle) and of the helicity (right) at the latest time of computation, with vertical columns shrouded by small-scale isotropic vortices.

and for the three LES runs which are identical except for the resolution of the grid used in the LES. For none of these runs is a global energy increase discernible (except for the initial phase adjustment to rotation), since the inverse cascade of energy is barely resolved, with a forcing at $k_F = 4$. The initial growth, up to $t \approx 4.5$, is remarkably similar for all runs, presumably because this phase is dominated by waves with little need for parameterization, whereas differences become discernible afterwards. All LES runs underestimate the energy, by roughly up to 15%, and overestimate the helicity (not shown). Neither the injection rate nor the dissipation differs significantly from run to run, except for a phase difference in the oscillations, and thus the Zeman wavenumbers computed for all runs are quite close. These oscillations linger on over time, a phenomenon likely related to the excitation of waves when rotation is turned on [72], but note that all LES runs exhibit a persistent delay with respect to the DNS. It would be of interest to identify the origin of this discrepancy.

The phenomenological prediction for turbulence in the presence of rotation is that $E(k) \sim k^{-e}$, $H(k) \sim k^{-h}$, with $e + h = 4$ at scales where rotation prevails, and $E(k) \sim H(k) \sim k^{-5/3}$ beyond the Zeman scale when isotropy is recovered. In the light of this, we show $k^{10/3} E(k) H(k)$ on the right of figure 1 (top). All spectra are in overall good agreement until the Zeman wavenumber $\approx$30, at which there is a break in the spectra, and they evolve towards a dual Kolmogorov cascade in the DNS [73]. This break in the spectra is visible for all LES runs, but clearly too accentuated for the lower resolutions. The Kolmogorov law for $E(k)$ and $H(k)$ is well recovered, whereas the steeper spectrum in the DNS is not accurate except at the highest-resolution LES, although the transition between the two is well marked in all runs. The fine-tuning between waves and nonlinear steepening due to advection may need an even higher resolution in the LES, in part because the fit to the spectrum catches the Kolmogorov part but perhaps misses, in the evaluation of transport coefficients, the large-scale steeper part. Note that the error in the global energy has to be put in perspective, realizing the enormous saving in computation time, $\approx (3172/512)^4 > 1400$ for the 512^3 LES (and more so for the lower-resolution LES). Finally, at the bottom of figure 1 are given visualizations of the 3072^3 run at the final time of the computation, with a 2D cut of the vertical component of the velocity (left), and 3D perspective views of the rms vorticity (middle) and helicity (right). When compared to a similar imaging for a run for which the Zeman scale is not resolved, the vertical structures appear more fuzzy, as small-scale isotropic vortices are wrapped around the maximally helical columns.

In view of these results, as with those given in [2] for tests of the same LES but against a DNS at lower resolution and not resolving the Zeman scale, we can conclude that the LES model can reproduce well the dynamics of the anisotropic large scales even in complex flows with different scaling behaviors at different scales. Using this LES, we now show in figure 2 the energy spectrum at different times for a run with $Re \approx 6.2 \times 10^4$ and $Ro = 0.014$, forced at $k_F = 7$ on a grid of 192^3 points; the initial conditions are those of a fully developed turbulent flow without rotation. As time evolves, the small-scale range becomes steeper, and the inverse cascade builds up progressively towards scales larger than the forcing scale. At the final time, the energy has reached

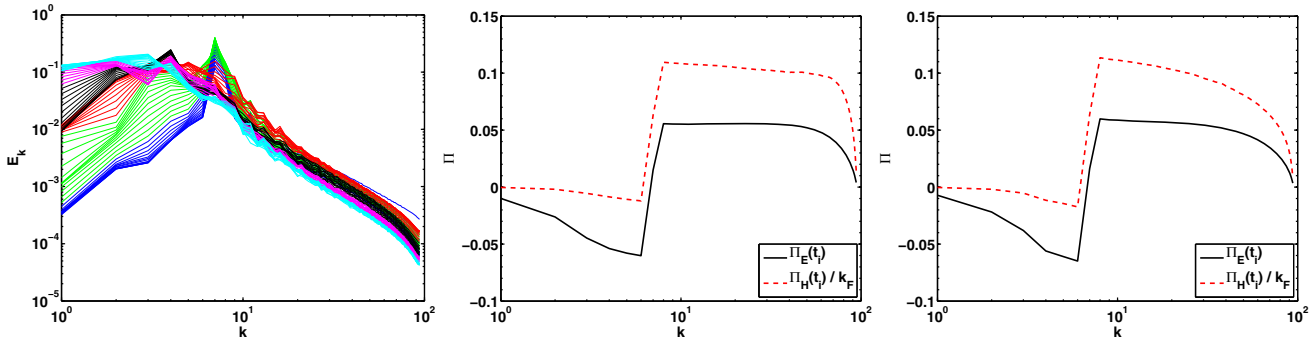

Figure 2. Left: temporal evolution (from dark blue, through green, red, black, mauve to cyan) of the energy spectrum for a run with $Re \approx 6.2 \times 10^4$, $Ro = 0.014$. One sees that the effect of rotation is to populate the large scales at the expense of the small scales which are depleted. Energy (solid black) and helicity (red dashed) spectral fluxes at the end of the computation for two runs with (middle) high and (right) moderate (four times smaller) Re, but with otherwise comparable Rossby numbers and numerical resolutions. Constancy of the flux of energy and helicity to the small scales only occurs at the higher Reynolds number.

the largest available scale (no large-scale friction is used). The energy and helicity fluxes are also shown for the same run in figure 2, the latter normalized by the forcing scale. We observe, as already mentioned in [72, 73], a dominance of the helicity flux to small scales, and of the energy flux of opposite sign to large scales, the helicity flux being negligible for scales larger than L_F. Lastly, on the right in figure 2 are these fluxes for a run with the same Rossby number but a Reynolds number four times smaller, in which case the constancy of the fluxes is not as well realized.

4. The inverse cascade of energy in rotating turbulence

When solid-body rotation is imposed on the flow, the interactions between inertial waves and nonlinear eddies lead to a slowing down of the energy transfer to small scales and to a steeper spectrum that can be modeled using a simple phenomenological argument which incorporates the interactions between eddies and waves [5, 36, 117]. Furthermore, when helical forcing is used, another scaling law arises because of the dominance of the helicity cascade to small scales [72, 73, 88]. Moreover, the direct cascade of energy is found to be scale invariant, and in fact conformal invariant [102], a stronger local property involving transformations that preserve angles, and this again connects the 2D turbulence problem with other quasi-2D flows.

The inverse energy cascade to scales larger than the forcing scale in rotating turbulence has been studied using numerical simulations with hyper viscosity in [96], where it was shown that it coexists with the direct cascade of energy. It was also found that most of the energy resides in the 2D modes, i.e. those with $k_z = 0$ [97]. A further exploration using the so-called reduced models at moderate Rossby number $\sim 10^{-1}$ showed that only the models that include near resonances reproduce well the (moderately resolved) DNS flows [98]. (See [47, 54] for the statistical mechanics case.)

New computations of the inverse cascade of energy in 3D rotating flows, for both non-helical and helical forcing, and for 2D versus 3D forcing, are being conducted at present [92]; they use the spectral LES tested in the preceding section, at resolutions of 256^3 grid points, and some DNS are in the planning stage as well. These investigations lead to the conclusion that the way the forcing occurs, putting more or less weight on 2D modes (i.e. forcing in the horizontal plane) versus fully 3D modes, is the main parameter of the problem and breaks the universality, as already found in [98] when only a subset of the triadic interactions as considered.

Given a random isotropic forcing function $\mathbf{f}_{\mathrm{RND}}(\mathbf{k})$ centered in a narrow band around k_F and with a certain relative helicity, one can prescribe in simulations the amount of 2D versus 3D forcing by defining a new forcing:

$$\mathbf{f}_{\mathrm{ANI}}(\mathbf{k}, k_F) = \left(1 - \frac{k_z}{k_F}\right)^{\beta} \mathbf{f}_{\mathrm{RND}}(\mathbf{k}, k_F),$$

with the parameter β controlling how much energy is injected in 2D modes, $\beta = 0$ corresponding to isotropic forcing. One can then study the scaling of the energy in 2D and 3D modes by decomposing E into its 3D component, $E_{3\mathrm{D}}$, with $k_z \neq 0$, and its 2D components for $\mathbf{u}_\perp$ (of energy $E_\perp$) and u_z (of energy E_w), both with $k_z = 0$, i.e. for the subset of modes with no variation in the direction of the rotation, with $E_{2\mathrm{D}} = E_\perp + E_w$.

Figure 3 shows the evolution of the 2D energy spectrum for a random flow with $\beta = 1$ (i.e. for slightly anisotropic forcing) and with $k_F = 40$. It grows with time at large scale and dominates the 3D component at all times except in the onset phase; it has almost reached the gravest mode at the final time, following a $k_\perp^{-3}$ law. This result is also found for several other runs, except when the forcing is strongly anisotropic (e.g. for the ABC forcing or for a random forcing with $\beta = 3$). In the latter cases, a $k_\perp^{-5/3}$ is obtained in the inverse cascade of 2D energy [92]. In figure 3 (middle), we show the relative helicity for a helical run as a function of wavenumber. It is maximal (by construction) at the forcing wavenumber and appears to decrease slowly in the direct cascade and sharply in the inverse cascade of energy: helicity does not efficiently follow the energy to large scales, as was already clear when plotting the fluxes of helicity and energy (see figure 2 and [72]). This is also noticeable when examining the spectrum of 2D helicity given on the right in figure 3 for several times as well during the inverse cascade phase for the energy; in these units, the spectrum is flat, indicating that no cascade to large scale is taking place for the helicity, corroborating the observation made when looking at the flux of helicity.

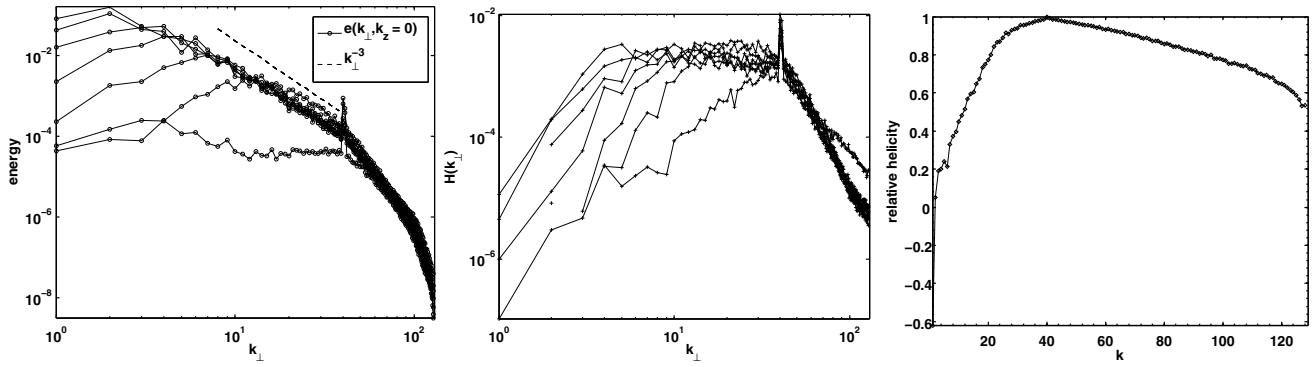

Figure 3. Left: 2D energy spectrum $e(k_\perp, k_z = 0)$ for various times for a non-helical random forcing with $\beta = 1$; note the build-up towards a $k_\perp^{-3}$ law. Middle: 2D helicity spectra $h(k_\perp, k_z = 0)$ as a function of time for a $\beta = 3$ maximal helicity forcing. Right: spectrum of relative helicity, the same run and the same times; note its sharp decrease for large scales.

We finally note that the dynamics resulting from an ABC forcing behaves in a unique way: the 2D modes still follow a $\sim k_\perp^{-5/3}$ spectrum; however, in this case alone, the isotropic energy spectrum in the inverse cascade range follows a k^{-1} law, due to strong anisotropy in the forcing and with a strong influence of shear at large scales [92].

5. Conclusions

In this paper, after reviewing recent results on 2D turbulence, we tested a previously developed sub-grid scale model against a large DNS of rotating turbulence performed on a grid of 3072^3 points. We showed, in particular, that the transition from a large-scale anisotropic to a small-scale isotropic inertial range is well reproduced in the sub-grid scale model, granted that the LES is sufficiently resolved.

We then used the model to confirm that for rotating turbulence, the inverse cascade of energy has two different scaling according to how anisotropic the forcing is [92], with shear moreover playing an important role in the strongly anisotropic case of the ABC flow, which is also fully helical. In that case, the presence of large-scale shear leads to a k^{-1} scaling for the total energy, while the slow modes still follow a $k_\perp^{-5/3}$ law.

A k^{-1} spectrum was also found in 2D fluid turbulence in the inverse cascade when decomposing the flow into its coherent part and the remainder of the flow, for the latter component; this took place both in the decay case [8] and in the forced case [30]. Such a shallow spectrum was attributed to the large-scale structure advecting passively an incoherent noise. It has also been advocated that the Fourier energy spectrum of the inverse cascade can in fact be shallow, namely again $E(k) \sim k^{-1}$, on the basis of nonlinear interactions with the stochastic small-scale vortices [80]; similarly, using Clebsch variables and using a weak turbulence closure procedure that, when dealing with four-wave interactions, leads to two different steady-state solutions [114], again a k^{-1} spectrum may emerge.

It remains to be seen whether other strongly anisotropic flows behave in a similar fashion; this could be examined, for example, by taking a higher value of the parameter β in the random forcing function introduced into the preceding section. Indeed, it appears that, depending on the extent of anisotropy in the external forcing function, shear may be introduced in to the flow, thereby altering the nature of the energy exchange between scales. In this context, it is worth noting that helicity and strong shear can be coupled, as observed in the atmosphere, for example, in the context of tornado and hurricane dynamics in the vicinity of deep convective cells [64, 77]. The presence of helicity in such large-scale systems can be attributed to the combined effects of stratification and rotation, as first modeled in [46] using geostrophic balance; this is linked to thermal winds, i.e. to vertically sheared horizontal velocities due to horizontal temperature gradients, as recently confirmed by a parametric numerical study [68].

The non-uniqueness of the scaling in the inverse cascade of rotating turbulence, for both the 2D and the 3D spectra, clearly needs further investigation. Quasi-2D flows show a richness of behavior and the detailed properties of the inverse cascade to large scales can vary according to the flow setup considered. It is likely that such a diversity will be unraveled as well for 3D flows in the presence of rotation, as already shown in [98] using a model that preserves a subset of triadic interactions. The lack of universality of the inverse cascade discussed here is well known (for a recent investigation see [16]). It can be put in the more general context of breaking of symmetries, leading to non-universality; it has also been demonstrated numerically for inverse cascades in other physical systems, such as for the nonlinear Schrödinger (Gross–Pitaevsky) model of nonlinear optics or superfluid turbulence or for non-random forcing exciting a particular instability mode [110].

Turbulent flows in the presence of stratification display vertical dispersion, which cannot be simply modeled by a random walk due to both the structures present in the flow and to wave propagation and their interactions [63]; such waves also undergo enhanced dissipation, as studied experimentally for example in the context of tidal flows over sloped and corrugated oceanic floors [49]. Similarly, of particular interest is the well-documented capacity of such turbulent flows in geophysics and astrophysics, as well as in engineering, to enable chemical reactions through altering the contact rates, as in combustion or in the production of ozone in the lower troposphere because of pollution. In the context of gravity and inertial waves due to both rotation and stratification in geophysics, concepts of statistical mechanics of ideal (non-dissipative) flows can be quite useful in understanding

the overall behavior of such flows in the 2D case, on a plane or on the sphere, for the so-called beta-plane turbulence, or in the geostrophic or baroclinic cases (see, e.g. the review in [47]). This leads to wave coupling and breaking and to shear instabilities, sometimes in isolated, intermittent but powerful events, and this results in extended Fourier spectra of the basic variables and therefore in enhanced dissipation and mixing. The energy and the seeds required for these events to occur may come from the wave fields that are perturbed or from winds and interactions with topography and bathymetry. However, a detailed understanding of, say, the interior of the ocean and how mixing occurs in such conditions still eludes us [20, 50], and yet such an understanding is a central element of advanced modeling of these flows, on both the short (meteorological) and the long (climatological) term. For example, mixing in coastal currents plays a role in the global oceanic circulation, in particular in meso-scale variability, due to their high level of instability and their ability to create fronts [43] and alter the patchiness of phyto-plankton and that of other tracers. It is a combination of methodologies (observations, experiments, numerical simulations, modeling and theory) that will enable us to progress significantly not only in a given field but also by comparing and contrasting different flows in different environments.

Acknowledgments

This work was sponsored by a National Science Foundation (NSF) cooperative agreement of the National Center for Atmospheric Research (NCAR) and by NSF/CMG grant 1025183. Computer time was provided by the NSF TeraGrid projects ASC090050 and TG-PHY100029.

References

[1] Babin A, Mahalov A and Nicolaenko B 1996 *Eur. J. Mech.* B **15** 291
[2] Baerenzung J, Rosenberg D, Mininni P D and Pouquet A 2011 *J. Atmos. Sci.* **68** 2757
[3] Batchelor G K 1969 *Phys. Fluids* **12** II-233
[4] Berhanu M *et al* 2007 *Europhys. Lett.* **77** 59001
[5] Bellet F *et al* 2006 *J. Fluid Mech.* **562** 83
[6] Benzi R *et al* 2003 *Phys. Rev.* E **68** 016308
[7] Bernard D, Boffetta G, Celani A and Falkovich G 2006 *Nature Phys.* **2** 124
[8] Beta C, Schneider K and Farge M 2003 *Commun. Nonlinear Sci. Numer. Simul.* **8** 537
[9] Biferale L, Musacchio S and Toschi F 2012 *Phys. Rev. Lett.* **108** 164501
[10] Biglari H, Diamond P H and Terry P W 1990 *Phys. Fluids B* **2** 1
[11] Boffetta G and Musacchio A 2010 *Phys. Rev.* E **82** 016307
[12] Boffetta G, De Lillo F and Musacchio S 2011 *Phys. Rev.* E **83** 066302
[13] Boffetta G and Ecke R 2012 *Annu. Rev. Fluid Mech.* **44** 427
[14] Borue V 1993 *Phys. Rev. Lett.* **71** 3967
Borue V 1994 *Phys. Rev. Lett.* **72** 1475
[15] Bouchet F and Simonnet E 2009 *Phys. Rev. Lett.* **102** 094504
[16] Bourouiba L, Straub D N and Waite M L 2012 *J. Fluid Mech.* **690** 129
[17] Bracco A and McWilliams J 2010 *J. Fluid Mech.* **646** 517
[18] Bruneau C H and Kellay H 2005 *Phys. Rev.* E **71** 046305
[19] Carnevale G F *et al* 1991 *Phys. Rev. Lett.* **66** 2735
[20] Cavaleri L, Fox-Kemper B and Hemer M 2012 Wind-waves in the coupled climate system *Bull. Am. Met. Soc.* **93** 1651
[21] Celani A, Musacchio S and Vincenzi D 2010 *Phys. Rev. Lett.* **104** 184506
[22] Cencini M, Muratore-Ginanneschi P and Vulpiani A 2011 *Phys. Rev. Lett.* **107** 174502
[23] Chakraborty S 2007 *Eur. Phys. Lett.* **79** 14002
[24] Chan C-K, Mitra D and Brandenburg A 2012 *Phys. Rev.* E **85** 036315
[25] Chavanis P and Sommeria J 1996 *J. Fluid Mech.* **314** 267
[26] Chen Q, Chen S-Y and Eyink G 2003a *Phys. Fluids* **15** 361
[27] Chen S-Y *et al* 2003b *Phys. Rev. Lett.* **91** 214501
[28] Chen S-Y *et al* 2006 *Phys. Rev. Lett.* **96** 084502
[29] Chertkov M, Kolokolov I and Vergassola M 1998 *Phys. Rev. Lett.* **80** 512
[30] Chertkov M *et al* 2007 *Phys. Rev. Lett.* **99** 084501
[31] Childress S and Gilbert A 1995 *Stretch, Twist, Fold: The Fast Dynamo* (Berlin: Springer)
[32] Colquhoun J and Riley P 1996 *Weather Forecast.* **11** 360
[33] Craya A 1958 Contribution à l'analyse de la Turbulence Associée à des Vitesses Moyennes *Publ. Sci. Tech. Min. Air* **345**
[34] Danilov S and Gurarie D 2001 *Phys. Rev.* E **63** 061208
[35] Dmitruk P, Mininni P D, Pouquet A, Servidio S and Matthaeus W H 2011 *Phys. Rev.* E **83** 066318
[36] Dubrulle B and Valdetarro L 1992 *Astron. Astrophys.* **263** 387
[37] Elhmaidi D, von Hardenberg J and Provenzale A 2005 *Phys. Rev. Lett.* **95** 014503
[38] Eyink G and Sreenivasan K 2006 *Rev. Mod. Phys.* **78** 87
[39] Fer I 2006 *Deep Sea Res. II* **53** 77
[40] Fischer P and Bruneau C-H 2009 *Phys. Fluids* **21** 065109
[41] Fox-Kemper B *et al* 2011 *Ocean Model.* **39** 61
[42] Frisch U, She Z S and Sulem P-L 1987 *Physica* D **28** 382
[43] Gula J and Zeitlin V 2010 *J. Fluid. Mech.* **659** 69
[44] Héas P *et al* 2012 *Tellus* A **64** 10962
[45] Herring J 1974 *Phys. Fluids* **17** 859
[46] Hide G 1976 *Geophys. Fluid Dyn.* **7** 157
[47] Holloway G 1986 *Annu. Rev. Fluid Mech.* **18** 91
[48] Hossain M, Matthaeus W and Montgomery D 1983 *J. Plasma Phys.* **30** 479
[49] Ibragimov R, Yilmazb N and Bakhtiyarovb A S 2011 *Mech. Res. Commun.* **38** 261
[50] Ivey G, Winters K and Koseff J 2008 *Annu. Rev. Fluid Mech.* **40** 169
[51] Julien K *et al* 2012 Statistical and physical balances in low Rossby number Rayleigh–Bénard convection *Geophys. Astrophys. Fluid Dyn.* at press
[52] Jun Y and Wu X L 2005 *Phys. Rev.* E **72** 035302
[53] Jun Y, Zhang J and Wu X L 2006 *Phys. Rev. Lett.* **96** 024502
[54] Jung S, Morrison P and Swinney H 2006 *J. Fluid Mech.* **554** 433
[55] Kraichnan R H 1967 *Phys. Fluids* **10** 1417
[56] Kraichnan R H 1971 *J. Fluid Mech.* **47** 525
[57] Kraichnan R H 1973 *J. Fluid Mech.* **59** 745
[58] Kraichnan R H 1976 *J. Atmos. Sci.* **33** 1521
[59] Kraichnan R H and Montgomery D 1980 *Rep. Prog. Phys.* **43** 547
[60] Kritsuk A, Norman M and Padoan P 2006 *Astrophys. J.* **638** L25
[61] Lamriben C, Cortet P-P and Moisy F 2011 *Phys. Rev. Lett.* **107** 024503
[62] Leith C E 1968 *Phys. Fluids* **11** 671
[63] Lindborg E and Brethouwer G 2008 *J. Fluid Mech.* **614** 303
[64] Levina G and Montgomery M 2010 *Dokl. Earth Sci.* **434** 1285
[65] Lindborg E and Alvelius K 2000 *Phys. Fluids* **12** 945
[66] Maassen S R, Clercx H J H and van Heijst G J F 2003 *J. Fluid Mech.* **495** 19

[67] Maltrud M E and Vallis G 1991 *J. Fluid Mech.* **228** 321
[68] Marino R, Mininni P D, Rosenberg D and Pouquet A 2012 Geostrophic balance and the emergence of helicity in rotating stratified turbulence *Phys. Rev. Lett.* submitted (arXiv:1211.3159)
[69] Matthaeus W H *et al* 2008 *Phys. Rev. Lett.* **100** 085003
[70] McWilliams J C 1984 *J. Fluid Mech.* **146** 21
[71] Mininni P D, Alexakis A and Pouquet A 2009 *Phys. Fluids* **21** 015108
[72] Mininni P D and Pouquet A 2010 *Phys. Fluids* **22** 035105
Mininni P D and Pouquet A 2010 *Phys. Fluids* **22** 035106
[73] Mininni P D, Rosenberg D and Pouquet A 2012 *J. Fluid Mech.* **699** 263
[74] Mininni P D and Pouquet A 2011 Ergodicity and inverse cascades in freely decaying two-dimensional turbulence *Phys. Rev.* E submitted
[75] Mishra P K and Verma M K 2010 *Phys. Rev.* E **81** 056316
[76] Moffatt H K and Tsinober E 1992 *Annu. Rev. Fluid Mech.* **24** 281
[77] Molinari J and Vollaro D 2008 *Mon. Weather Rev.* **136** 4355
[78] Montgomery D C *et al* 1992 *Phys. Fluids* A **4** 3
[79] Nastrom G D and Gage K S 1985 *J. Atmos. Sci.* **42** 950
[80] Nazarenko S and Laval J P 2000 *J. Fluid Mech.* **408** 301
[81] Bell T L and Nelkin M 1977 *Phys. Fluids* 20:345
[82] Ngan K, Straub D N and Bartello P 2004 *Phys. Fluids* **16** 2918
[83] Onsager L 1949 *Supplemento al vol VI, Series IX del Nuovo-Cimento* **2** 279
[84] Paret J and Tabeling P 1998 *Phys. Fluids* **10** 3126
[85] Pasquero C and Falkovich G 2002 *Phys. Rev.* E **65** 056305
[86] Podvigina O and Pouquet A 1994 *Physica* D **75** 475
[87] Pouquet A, Frisch U and Chollet J P 1983 *Phys. Fluids Lett.* **26** 877
[88] Pouquet A and Mininni P D 2010 *Phil. Trans. R. Soc.* **368** 1635
[89] Schmeits M J and Dijkstraa H A 2001 *J. Phys. Oceanogr.* **31** 3435
[90] Schorghofer N 2001 *Phys. Rev.* E **61** 6572
[91] Scott R K 2007 *Phys. Rev.* E **75** 046301
[92] Sen A, Rosenberg D, Pouquet A and Mininni P D 2012 Anisotropy and non-universality in scaling laws of the large scale energy spectrum in rotating turbulence *Phys. Rev.* E submitted (arXiv:1203.5131)
[93] Servidio S, Wan M, Matthaeus W H and Carbone V 2010 *Phys. Fluids* **22** 125107
[94] Shats M G, Xia H, Punzmann H and Falkovich G 2007 *Phys. Rev. Lett.* **99** 164502
[95] Smith L and Yakhotn V 1994 *J. Fluid Mech.* **274** 115
[96] Smithn L, Chasnovnn J and Waleffenn F 1996 *Phys. Rev. Lett.* **77** 2467
[97] Smith L and Waleffe F 1999 *Phys. Fluids* **11** 1608
[98] Smith L and Lee Y 2005 *J. Fluid Mech.* **535** 111
[99] Sommeria J 1986 *J. Fluid Mech.* **170** 139
[100] Sukoriansky S, Galperin B and Chekhlov A 1999 *Phys. Fluids* **11** 3043
[101] Tabeling P 2002 *Phys. Rep.* **362** 1
[102] Thalabard S *et al* 2011 *Phys. Rev. Lett.* **106** 204503
[103] Teitelbaum T and Mininni P D 2011 *Phys. Fluids* **23** 065105
[104] Tran C V and Bowman J 2003 *Physica* D **176** 242
[105] Valet J-P, Meynadier L and Guyodo Y 2005 *Nature* **435** 802
[106] Vallgren A and Lindborg E 2010 *J. Fluid Mech.* **656** 448
[107] Vallgren A and Lindborg E 2011 *J. Fluid Mech.* **667** 463
Vallgren A and Lindborg E 2011 *J. Fluid Mech.* **671** 168
[108] Verma M 2011a Variable enstrophy flux and energy spectrum in two-dimensional turbulence with Ekman friction *Preprint* IIT, Kanpur, India
[109] Verma M 2011b Variable energy flux in quasi-static MHD turbulence *Preprint* IIT, Kanpur, India
[110] Vladimirova N, Derevyanko S and Falkovich G 2012 *Phys. Rev.* E **85** 010101
[111] Waleffe F 1992 *Phys. Fluids* A **4** 350
[112] Waleffe F 1993 *Phys. Fluids* A **5** 677
[113] Xia H, Byrne D, Falkovich G and Shats M 2011 *Nature Phys.* **7** 321
[114] Yakhot V and Zakharov V 1993 *Physica* D **64** 379
[115] Yang Y T, Su W T and Wu J Z 2010 *J. Fluid Mech.* **662** 91
[116] Yin Z, Montgomery D C and Clercx H J 2003 *Phys. Fluids* **15** 1937
[117] Zhou Y 1995 *Phys. Fluids* **7** 2092